CHAPTER 6
Ice Force on Structures

6-1. Introduction

a. Any structure placed in an environment where the presence of ice is a hazard to its integrity and stability needs to be designed to withstand the forces generated by ice moving against it. A designer should also consider how the cold may affect the intended operations of a structure, because freezing of ice may hinder some of the normal warm weather operations. These guidelines are intended for structures placed in inland waters, e.g., lakes, rivers, and coastal waters. To estimate ice forces on an offshore structure see API (1995).

b. An ice sheet moves under the influence of shear stresses imparted by wind and water and by thermal expansion (as long as the ice sheet is intact). It transmits the accumulated forces to a structure situated in its path. The shear drag forces attributable to wind and water can be transmitted over large distances through an intact ice cover. In many situations, these environmental forces can be large, and the ice sheet fails during its interaction with a structure. The ice failure process limits the large environmental force being transmitted to the structure. Unless the environmental forces can be estimated with confidence to be small, the methodology to estimate ice forces from floating ice is generally to determine the forces required to fail an ice sheet in the vicinity of a structure. An ice sheet fails by crushing, splitting, bending, buckling, or a combination of these modes. For a given failure mode and structure shape, theoretical formulations or experimental results, along with ice properties, are used to estimate the forces required to fail an ice sheet. The forces are estimated for one, two, or all possible failure modes, and the failure mode with the lowest estimated force is assumed to occur at the ice–structure interface. At times, it may be necessary to conduct model tests to simulate an ice–structure interaction to determine the interaction forces. Attention should also be given to the clearance of broken ice pieces, because the advancing ice sheet will interact with the broken pieces if they accumulate in front of the structure. It is also possible that the accumulation of broken ice pieces may freeze together to form a grounded collar, which may provide some protection from further ice movement.

c. In situations where an ice cover is made up of drifting ice floes, the impact of these floes causes a horizontal force on a structure. (Although impact from a drifting iceberg falls into this category, we will limit our discussion to drifting ice floes.) The forces generated when ice floes strike a structure depend on the mass and the initial velocity of the floes. If the kinetic energy of the moving ice floes is greater than the work done in failing the ice along the entire width of the structure, the design force is then limited by the ice failure processes mentioned above. If the kinetic energy and the momentum of drifting ice floes are small, resulting in indentation of the structure into the ice floes over a part of its width, ice forces are estimated from balancing the momentum and the energy before and after an impact.

d. The methodology given in this Manual for estimating ice forces is based on the results of theoretical and experimental research in ice mechanics and measurements of ice forces in the field. Most recently, our understanding of processes active during crushing of ice at various indentation speeds has been increased. Data on measured ice forces on large structures have re-

cently been published. Except for the recommended values of effective pressure, the Corps guidelines for ice forces on structures are almost the same as those of the American Association of State Highway and Transportation Officials (AASHTO 1994), which in turn were adopted from the Canadian Standards Association (CSA 1988, 2000). Montgomery et al. (1984) provide the background information for the recommendations in CSA (1988). The CSA (2000) and the AASHTO (1994) codes consider dynamic and static loads on bridge piers located in rivers, lakes, and coastal waters. The dynamic loads develop when moving ice fails against a pier during spring breakup, or when currents and wind move ice sheets past piers at other times of the year. The static loads are generated by thermal expansion or contraction of the ice and by fluctuations in the water levels.

6-2. Mechanical Properties of Ice

a. Introduction.

(1) Because the forces necessary to fail an ice sheet depend on the mechanical properties of ice, the mechanical properties of the freshwater and sea ice are briefly reviewed below before methodologies to estimate the ice forces on a structure are given. Ice is a unique material. In the temperature range under which it is normally encountered, it is very close to its melting point. Ice can creep with very little applied stress, or it can fracture catastrophically under a high strain rate.

(2) There are two primary ways to categorize ice. One is based on the melt from which the ice is grown (freshwater or sea water), and the other is based on the size of the ice blocks (i.e., large ice floes or accumulations of broken ice in a random ice rubble). The conditions under which ice forms will determine its grain structure, with common forms being frazil ice, columnar ice, discontinuous columnar ice, and granular ice. Both the porosity within the ice and the grain structure significantly influence the mechanical properties of the ice. Various books (e.g., Michel 1978, Ashton 1986, Cammaert and Muggeridge 1988, Sanderson 1988) cover the subjects of formation and types of ice, as well as ice properties.

(3) The porosity attributable to brine and air pockets affects the ice properties. The brine volume ν_b ($^o/_{oo}$) is obtained from the following relation (Frankenstein and Garner 1967):

$$\nu_b = S_i\,(0.532 + 49.185/|T|) \tag{6-1}$$

where S_i ($^o/_{oo}$) = salinity, T (°C) = temperature of the ice, and the symbol $^o/_{oo}$ refers to parts per thousand.

(4) The porosity ascribable to air can be obtained from the following relation after the bulk density ρ of ice containing salt and air are measured (Cox and Weeks 1983)

$$V_a/\,V = 1\text{-}\rho/\rho_i + \rho S_i F_2(T)/F_1(T) \tag{6-2}$$

where

V_a = volume of air
V = bulk volume

ρ_i = density of pure ice
S_i = salinity of ice
$F_1(T)$ and $F_2(T)$ = functions of temperature derived from a phase equilibrium table (Cox and Weeks 1983) and given in Figure 6-1.

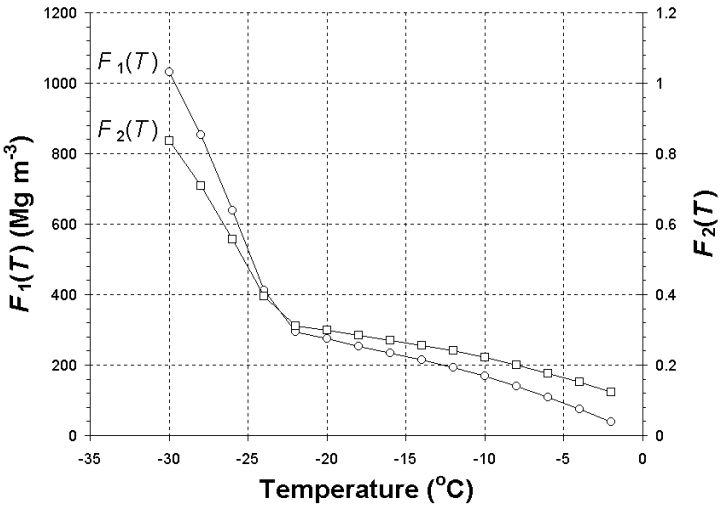

Figure 6-1. Plots of $F_1(T)$ and $F_2(T)$ with respect to temperature. To convert degrees C to degrees F use the following: ºF = ºC × 1.8 +32.

b. Compressive Strength. Values of the uni-axial compressive strength for ice range from 0.5 to 20 MPa (72.5 to 2900 psi). The strength is a function of strain rate, temperature, grain size, grain structure, and porosity. Analyses of strength measurements have shown that the strength increases with strain rate, up to a rate of 10^{-3} s^{-1} , whereupon the strength generally decreases at higher strain rates because of brittle fracture.

(1) In the lower strain rate range below 10^{-3} s^{-1}, the compressive strength of freshwater ice is given by (Sinha et al. 1987)

$$\sigma_c = 212\dot{\varepsilon}^{0.34} \quad (3.07 \times 10^4 \ \dot{\varepsilon}^{0.34}) \tag{6-3}$$

where σ_c is in MPa (psi) and $\dot{\varepsilon}$ is in s^{-1}.

(2) The above expression is for the compressive strength of ice at –10°C (263 K or 14ºF). The compressive strength at another temperature T(K) can be obtained by multiplying the strength at –10°C (14ºF) by a correction factor $[\exp\{(Q/R)(263–T)/(263T)\}]^{1/3}$, where Q = 65 kJ mol^{-1} (61.6 Btu mol^{-1}) (the activation energy for columnar ice) and R = 8.314 J mol^{-1} K^{-1} (1.986 Btu lb^{-1} mol^{-1} R^{-1}) (the universal gas constant).

(3) For sea ice, the following equations for compressive strength were derived from an analysis of over 400 small sample tests (Timco and Frederking 1990). These equations are:

$$\sigma_c = 37\dot{\varepsilon}^{0.22}\left[1-\left(\upsilon_T/270\right)^{0.5}\right] \text{ for horizontally loaded columnar sea ice} \quad (6\text{-}4)$$

$$\sigma_c = 160\dot{\varepsilon}^{0.22}\left[1-\left(\upsilon_T/200\right)^{0.5}\right] \text{ for vertically loaded columnar sea ice} \quad (6\text{-}5)$$

$$\sigma_c = 49\dot{\varepsilon}^{0.22}\left[1-\left(\upsilon_T/280\right)^{0.5}\right] \text{ for granular sea ice} \quad (6\text{-}6)$$

where $\dot{\varepsilon}$ is the strain rate in s^{-1}, and υ_T is the total porosity in the ice (brine and air) in parts per thousand. The range of strain rate for these equations is 10^{-7} to 10^{-4} s^{-1}. Above this strain rate, the ice can experience brittle failure with compressive strengths exhibiting a wide range of variability.

c. Flexural Strength. The flexural strength is generally lower than the compressive strength. Measurements on freshwater ice range from 0.5 to 3 MPa (72.5 to 435 psi), with an average of 1.73 MPa (for temperatures less than –5°C (23ºF) (Timco and O'Brien 1994). There is very little temperature or strain rate dependence, but there is a wide scatter in the measured flexural strength with higher values from smaller samples. At temperatures close to 0°C (32°F), the strength of freshwater ice can be essentially zero if solar radiation has caused pronounced "candling." For sea ice, Timco and O'Brien (1994) compiled the results of over 900 flexural strength measurements to obtain the following dependence of the flexural strength on the brine volume.

$$\sigma_f = 1.76e^{-5.88\sqrt{\upsilon_b}} \quad (255\,e^{-5.88\sqrt{\upsilon_b}}) \quad (6\text{-}7)$$

where σ_f is in MPa (psi) and ν_b is the brine volume fraction. The strength value for zero brine volume (1.76 MPa or 255.3 psi) agrees with the average value of 1.73 MPa (250.9 psi) determined from tests on freshwater ice.

d. Fracture Toughness. The fracture toughness depends on the loading rate and the ice type, with less variation ascribable to temperature and grain size. Typical values for freshwater ice range from 109 ± 8 kPa $m^{0.5}$ (0.01581 ± 0.00116 ksi $in.^{0.5}$), for columnar-grained S2 ice, to 151 ± 12 kPa $m^{0.5}$ (0.0219 ± 0.00174 ksi $in^{0.5}$)for granular ice (Weber and Nixon 1992). In-situ measurements of the fracture properties of lake ice and sea ice revealed that fracture toughness depends on the size of the specimen, and that its range is 50–250 kPa $m^{0.5}$ (0.00725 to 0.03626 ksi $in.^{0.5}$) (Dempsey et al. 1999a,b)

e. Elastic Modulus. Ice deformation involves elastic and creep processes, and the large-scale modulus is usually discussed in terms of an "effective modulus" that incorporates these processes. This modulus is a strong function of loading rate, temperature, and grain size and type. The values of elastic modulus range from approximately 2 GPa (2.9×10^5 psi) at low frequency loading to a high frequency value of 9 GPa (1.3×10^6 psi) (Sinha et al 1987, Cole 1995a,b).

f. Broken Ice Properties. Ice rubble is usually assumed to behave as a linear Mohr-Coulomb material, for which the shear stress τ and the normal stress σ_n on a failure plane are related by

$$\tau = c + \sigma_n \tan\phi \quad (6\text{-}8)$$

where c is the apparent cohesion and ϕ is the effective angle of internal friction. Recent studies (Prodanovic 1979, Ettema and Urroz-Aguirre 1991, Løset and Sayed 1993, Cornett and Timco 1996) have shown that the yield envelope is non-linear but can be approximated with a linear envelope for a limited range of conditions; that cohesion is negligible for unconsolidated rubble; that ϕ depends on the stress history and decreases with increasing pressure; that ϕ is less than the maximum angle of repose; and that ϕ depends on the strain path and pressure. Measured values of ϕ range from 20° to 45°.

6-3. Environmental Forces

a. Wind and Water Drag Forces. The drag force, caused by wind and water shear stresses on the top and bottom surfaces of an ice cover, can be estimated from the following expression:

$$F_d = C_d \rho A V^2 \tag{6-9}$$

where

C_d = drag coefficient
ρ = density of air or water
A = fetch area
V = velocity of air or water measured at a certain distance above or below an ice cover.

Typical values for C_d are 0.002 for a smooth ice cover, and 0.005 for a rough ice cover (Banke and Smith 1973). Typical values for the density of air and water are 1.3 and 1000 kg m^{-3} (0.08116 and 62.4 lb ft^{-3}), respectively. When sufficient information is available on the wind and water velocities and the fetch area, it may be possible to estimate the wind and water drag forces. However, it is difficult, in most cases, to estimate the fetch area that contributes directly to wind and water drag forces on a structure. In most situations, the estimates of wind and water drag force are greater than the force required to fail an ice sheet, and the ice failure process limits the force to that necessary to fail the ice against the structure. If wind and water drag forces can be estimated to be less than the ice failure force, the design force on the structure is taken to be the estimate of wind and water drag forces.

b. Thermal Ice Forces. Like other materials, ice expands with increasing temperature, and vice versa. However, unlike other materials, water expands when it changes phase from liquid to solid. These two properties, along with the creep of ice, explain the forces that develop when ice undergoes a temperature change. The temperature of ice changes because of conduction, radiation, and convection heat transfer at its surface. The depth to which temperature changes take place depends on the thickness of the ice cover, the presence or absence of snow on its top surface, and the environmental conditions (Michel 1970, 1978; Sanderson 1988).

(1) An unrestricted ice cover will expand as a whole in response to a change in temperature. While the top layer of the ice sheet expands as a result of the change in temperature, the bottom layer, because it undergoes no temperature change, restrains the top layer from expanding. This process causes the rate of expansion of the ice sheet to depend on the ice thickness. If

one edge of the ice cover is fixed to a shore, the rest of the ice sheet expands away from the shore. A structure placed some distance away from the shore will experience an ice force as a result of ice moving past it. For distances of shores on the order of 50 kilometers (31 miles), observers have measured the ice edge to move at a rate of about 0.9 meter (3 feet) per day (Strilchuk 1977).

(2) When an ice sheet is restricted from expansion from four or two sides, the confinement causes, respectively, biaxial or uniaxial stress (Sanderson 1984, 1988). The method of calculating thermal ice force in a confined ice sheet is as follows.

(*a*) Calculate temperature change as a function of depth, taking into account heat transfer by conduction, radiation, and convection.

(*b*) Calculate the rate of thermal expansion $\dot{\varepsilon}$ as if the ice would have been unconfined.

(*c*) Apply $-\dot{\varepsilon}$ at those depths to satisfy the assumption of complete restraint.

(*d*) Calculate the stress needed to deform the ice at those strain rates using one of Equations 6-3, 6-4, 6-5 or 6-6.

(*e*) Integrate the stress through the ice thickness to obtain force per unit width. In the case of a confined ice sheet having thicknesses greater than 0.5 meter (1.6 feet), the force per unit width does not strongly depend on ice thickness, because the ice layer below the 0.5-meter (1.6-foot) depth does not undergo a change in temperature and restricts expansion of ice in the top layer. Calculations of typical thermal ice force are in the range of 200–400 kN m^{-1} (1.5×10^5 to 2.95×10^5 lb_f ft^{-1}), whereas some of the measured values are in the range of 100–350 kN m^{-1} (7.4×10^4 to 2.6×10^5 lb_f ft^{-1}) (Sanderson 1984).

(3) The presence of cracks in an ice cover has a profound effect on thermally generated pressure within it. Metge (1976) observed three types of cracks: dry micro-cracks, wet micro-cracks, and wet large cracks. Dry micro-cracks are found at the top of an ice sheet and do not penetrate to the water below. Dry cracks close when an ice sheet thermally expands, and this closure of cracks does not result in a significant push against a structure. Wet micro-cracks are filled with water that freezes within them during cold periods. With repeated cooling, cracking, and freezing, a floating ice sheet can expand and push against a structure. Water within large wet cracks freezes only at the top surface during cold periods, and this creates a thin ice bridge across the gap of a crack. When the ice sheet expands during warm periods, these bridges are crushed, forming small pressure ridges along the crack.

(4) In summary, factors influencing thermally generated ice forces are the magnitude and the rate of temperature increase, heat transfer at the top surface and in the ice sheet, boundaries resisting expansion of an ice cover, creep relaxation of ice pressure, and dry and wet cracks. Several theories (Rose 1947; Belkov 1973; Drouin and Michel 1974; Xu Bomeng 1981, 1986; Fransson 1988) have been proposed to calculate the thermally induced ice force, and thermally induced ice pressures have been reviewed by several authors (Michel 1970, Kjeldgaard and Carstens 1980, Sanderson 1984). More recently, the predicted loads of these five theories were compared to the

results of a comprehensive field data set (Comfort and Abdelnour 1994). The comparison of each model with measured data showed a wide disparity, and no model predicted the measured loads (Timco et al. 1996). The disparity between theoretical estimates and measured values of thrust on dam walls may be attributed to changes in water levels in reservoirs and large wet cracks in the ice cover.

(5) In recent years, two measurement programs were launched.

(*a*) Comfort et al. (2000a,b) undertook a 9-year program, beginning in 1991–92, to measure the loads in the ice sheet adjacent to eight dam sites in Manitoba, Ontario, Quebec, and Labrador.

(*b*) Carter et al. (1998) undertook a 3-year program from 1995 to 1998 to measure the static ice forces in four reservoirs in central and northern Quebec. In both of these programs, changes in measured stress in an ice sheet correlated with changes in air temperature as well as water level.

(6) Carter et al. (1998) proposed that thermal ice loads are limited by the instability of ice blocks between two or three parallel cracks along a dam wall. Their measurements indicate that the ice thrust changes with increasing water level; the maximum values was about 150 kN m^{-1} (1.1×10^5 lb_f ft^{-1}). Comfort et al. (2000a, b) identified the importance of water level fluctuations to the ice loads on dam walls. They found the ice loads to be higher and more variable than those generated by thermal process alone when there were significant, but not excessive, water level changes. The range of ice thickness during their measurement program was 0.3–0.7 meters (1–2 feet). The maximum values of the measured line load resulting from thermal events with negligible change in water level at four dam sites in central and eastern Canada were in the range of 61 to 85 kN m^{-1} (4.5×10^4 to 6.3×10^4 lb_f ft^{-1}), with average value of 70 kN m^{-1} (5.2×10^4 lb_f ft^{-1}) (Comfort and Armstrong 2001). Similar values resulting from thermal events, combined with significant change in water level at four dams in central and eastern Canada, were in the range of 52 to 374 kN m^{-1} (3.8×10^4 to 2.8×10^5 lb_f ft^{-1}), with average value of 186 kN m^{-1} (1.4×10^5 lb_f ft^{-1}) (Comfort and Armstrong 2001). At Seven Sisters Dam in Manitoba, Comfort and Armstrong observed a significant reduction by a factor of 3–5 in ice thrust when the water level was lowered in early January by 45 centimeters (18 inches) and maintained there for the rest of the winter. More recently, they observed a similar reduction in ice thrust at the same site when the water level was lowered in late December or early January by 35 centimeters (14 inches) and then brought up to normal levels a few days later (Comfort and Armstrong 2001). These operations introduce large wet cracks and hinges in the ice sheets to limit the ice thrust to dam walls.

6-4. Forces Limited by Ice Failure

a. Introduction. The force resulting when a moving ice sheet and a structure interact is limited to the magnitude of force necessary to fail the ice sheet in crushing, bending, buckling, splitting, or a combination of these modes. In the following, procedures to estimate forces to fail ice sheets in the above mentioned modes are given.

(1) It is important to consider the magnitude of the area over which the ice forces act. The total force on the entire structure is important for designing foundations to resist sliding and overturning. Contact forces over small areas, or local contact pressures, are important for designing internal structural members and the external skin of a structure.

(2) The total ice force F on a structure of width D attributable to failure of an ice sheet of thickness h, as shown in Figure 6-2, is expressed in terms of the effective pressure p_e:

$$F = p_e D h \tag{6-10}$$

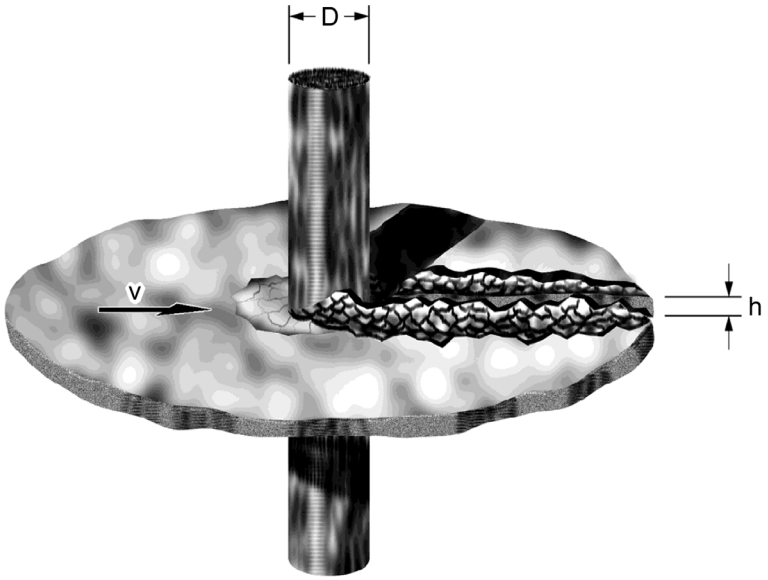

Figure 6-2. Total ice force *F* on a structure of width *D* attributable to failure of an ice sheet of thickness *h*.

(3) It is important to distinguish between the contact pressure acting over the ice–structure contact area and the effective pressure. Because the actual contact area between a structure and an ice sheet is either equal to or less than the nominal contact area (product of ice thickness and structure width), the contact pressure is either equal to or higher than the effective pressure. The relative speed of an ice sheet with respect to a structure is an important factor in determining the mode of ice failure and the resulting contact areas and effective pressures.

b. Crushing Failure. Ice crushing is one of the common modes of ice failure. Much work has been done to understand the processes taking place during ice crushing and to determine the forces generated at the interface. Because ice exists close to its melting temperature, its temperature strongly affects its properties. Ice at lower temperatures is stronger and also has more brittle characteristics. Ice creeps at low rates of loading, and it fails in a brittle manner at high loading rates. The complex behavior of ice depends on the temperature and the indentation speed. In engineering applications, one has to contend with both types of ice behavior.

(1) *General*. The effective pressure depends on the mode of ice crushing, which in turn depends on the rate of indentation, or the relative speed of an ice feature with respect to a structure.

(*a*) At low indentation rates, the ice deforms in creep, resulting in full contact and uniform pressure at the interface. During an interaction involving creep deformation of ice against a narrow structure, the force between an ice sheet and a structure increases gradually, attains a peak value, and then gradually reduces to a steady-state value at 50–60% of the peak force without any structural vibration (Sodhi 1991).

(*b*) At high rates of ice indentation against both narrow and wide structures, ice crushes continuously in a brittle manner, resulting in non-simultaneous, partial contact and non-uniform pressure over the nominal contact area. In this mode of crushing, the variations of force over small areas of a wide structure are large, but the summation of these forces across the whole width of a structure averages out the variations in local forces, resulting in smaller variations in the total ice force across the whole structure (Kry 1978, Sodhi 1998, Sodhi 2001). During continuous brittle crushing, the structure does not respond to rapid variations of the interaction forces, and its vibrations are not so severe because it deflects to a steady-state value in response to the average force.

(*c*) At intermediate speeds, the interaction between structural deformation and an advancing ice sheet produces alternating ductile and brittle crushing, resulting in ice force records taking a saw-tooth form. During each cycle of intermittent crushing, the advancing ice sheet deflects the structure while undergoing ductile deformation with increasing interaction force. When the ice sheet fails at a certain force level, the stored potential energy in the structure is released to move the structure back to its original position, resulting in high relative speeds and brittle crushing. When the transient oscillations decay, the cycle repeats, causing the structure to indent into the ice at varying speeds and to undergo either transient or steady-state vibrations (Jefferies and Wright 1988; Sodhi 1991, 1995, 2001).

(*d*) Figure 6-3 shows a map of ice crushing failure during interactions with rigid and compliant structures. During an ice interaction with a rigid structure, the ice fails in the ductile and brittle modes, and there is a sharp transition at an indentation speed that has been found to be close to 3 mm s^{-1} (0.01 ft s^{-1}) (Sodhi et al. 1998, Masterson et al. 1999). During an ice interaction with a compliant structure, the failure modes are ductile and brittle at low and high rates of indentation, respectively. At intermediate indentation speeds, the ice fails in the alternating ductile–brittle mode as a result of variable indentation rates into the edge of an ice sheet. Because of this, there are two transition speeds, ductile to intermittent and intermittent to continuous brittle crushing, during interactions with compliant structures. A video display of the interfacial pressure during three modes of ice crushing (ductile deformation, alternating ductile-brittle and continuous brittle crushing) can be seen at the following URL:
www.crrel.usace.army.mil/permanent/ice_crushing.

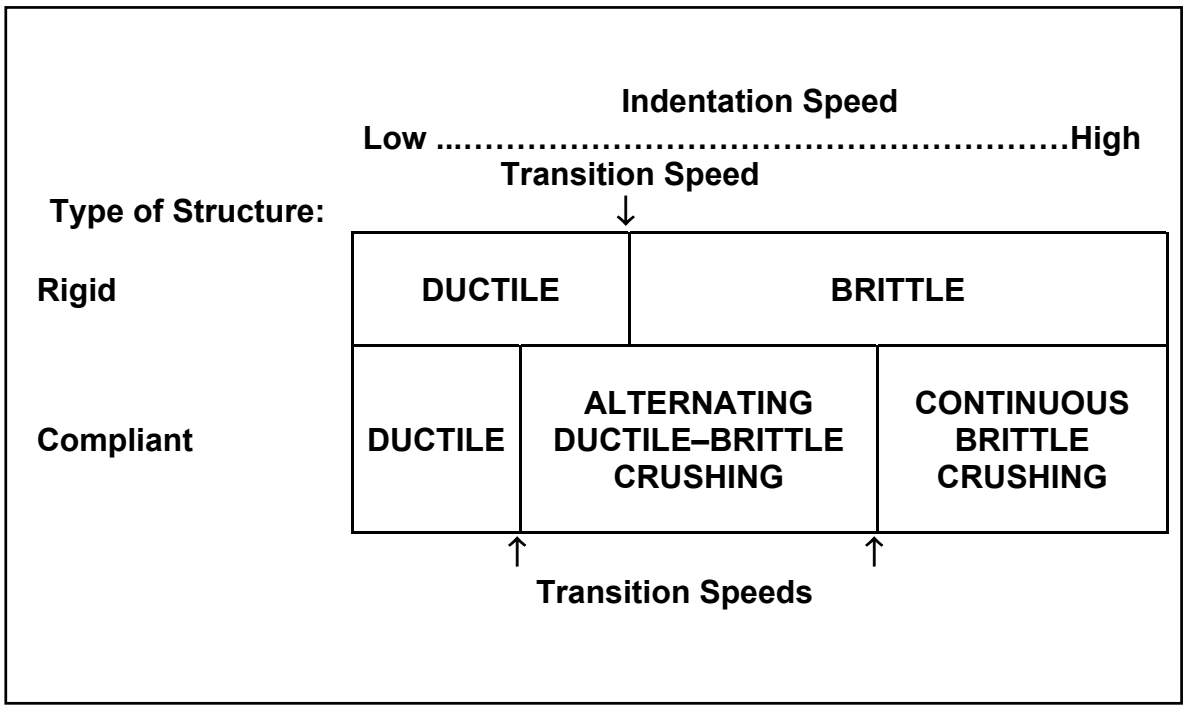

Figure 6-3. Failure map of ice crushing with respect to indentation speed and structural compliance.

(2) *Ductile Deformation of Ice.* Results of small-scale indentation tests on freshwater columnar ice (Michel and Toussaint 1977) indicate that the effective pressure for ductile (creep) deformation of ice at strain rates between 10^{-8} s^{-1} and 5×10^{-4} s^{-1} is

$$p_e = Cmk\sigma_0(\dot{\varepsilon}/\dot{\varepsilon}_0)^{0.32}, \tag{6-11}$$

where

C = indentation factor (=2.97)
m = shape factor (=1 for flat indentors)
k = contact factor (=1 for the first peak force, and =0.6 the for steady-state pressure after the first peak force)
σ_0 = uniaxial compressive strength of columnar ice at a temperature of –10°C (14ºF) and at a strain rate of $\dot{\varepsilon}_0=5\times10^{-4}$ s^{-1} (=7 MPa or 1015 psi)
$\dot{\varepsilon} = v/(4D)$ = empirically defined strain rate
v = indentation rate
D = indenter width.

This relation is similar to the strain rate dependence of uniaxial compressive strength for freshwater columnar ice.

(*a*) Figure 6-4 shows this comparison with good agreement between the plots of uniaxial compressive strength versus strain rate and the plots of effective indentation pressure divided

by 2.97 versus the empirical strain rate ($v/4D$). This expression may also be used for creep indentation of sea ice at any temperature by using the compressive strength of sea ice (Equations 6-2 to 6-4). While Figure 6-4 shows good correlation between effective indentation pressure and the uniaxial compressive strength of columnar ice at the appropriate strain rates, there is no confirmation whether the indentation factor and the empirical definition of strain rate ($v/4D$) will remain applicable for very large aspect ratios (D/h). Such confirmation is perhaps an impossibility because of creep buckling of floating ice sheets against wide structures at a lower effective pressure than that required for in-plane creep indentation.

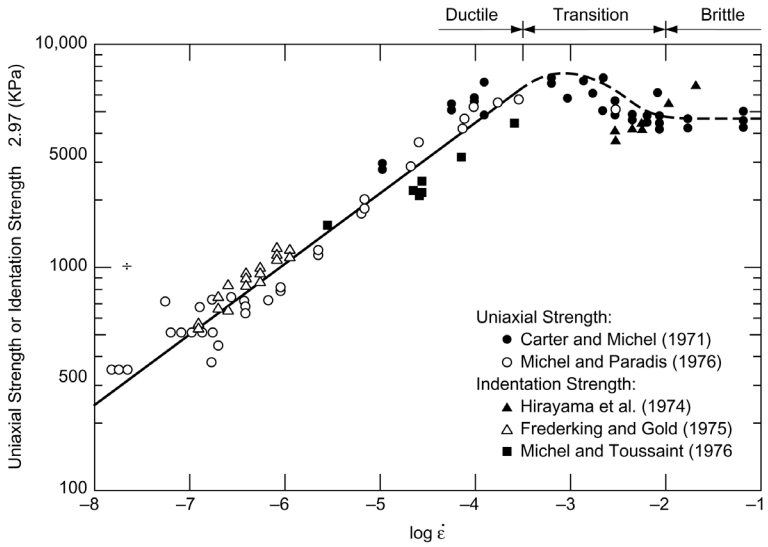

Figure 6-4. Plots of uniaxial compressive strength versus strain rate and the plots of effective indentation pressure divided by 2.97 versus the empirical strain rate ($v/4D$). (1 kPa × 0.145 = 1 psi.)

(*b*) Other methodologies to estimate the ice force ascribable to creep deformation of ice are the plastic limit analysis (Croasdale et al. 1977), and the reference stress method (Ponter et al. 1983, Sanderson 1988, also given in API 1995).

(3) *Brittle Crushing*. For edge indentation into floating ice sheets, the main characteristics of brittle crushing are the line-like contact in the middle third of the ice sheet thickness, the non-simultaneous contact in different parts of the contact line, and the non-uniform pressure in the contact area (Joensuu and Riska 1989, Sodhi et al. 1998, Sodhi 2001). This is caused by fracturing of ice at a high rate of loading, resulting in flaking failure of ice. Line-like contacts in the form of an "X" have also been observed during medium-scale indentation tests, in which spherical indentors were pushed into walls of ice at speeds greater than 3 mm s^{-1} (0.01 ft s^{-1}) (Frederking et al. 1990; Gagnon 1998). The results of full-scale measurements of ice forces, and medium- and small-scale tests indicate that the effective pressure for brittle crushing and for high aspect ratio (D/h) is in the range of 1 and 3 MPa (145 to 435 psi), which is less by a factor of three to four in comparison to the maximum pressure that develops at the high end of speed range for ductile deformation of ice over small areas or small aspect ratios (D/h). The reason for the reduction in effective pressure can be attributed to the actual contact area during brittle

crushing being much smaller than full contact during ductile deformation of ice. The following is an expression to estimate ice force F on a structure of width D for continuous brittle crushing of ice of thickness h at high indentation rates:

$$F=A_r pDh$$

where p is the effective pressure (1.5 to 2 MPa, or 217.5 to 290 psi) for brittle crushing of ice, and $A_r=(5h/D+1)^{0.5}$ is an empirical factor to account for the aspect ratio effect of high effective pressure over small aspect ratios.

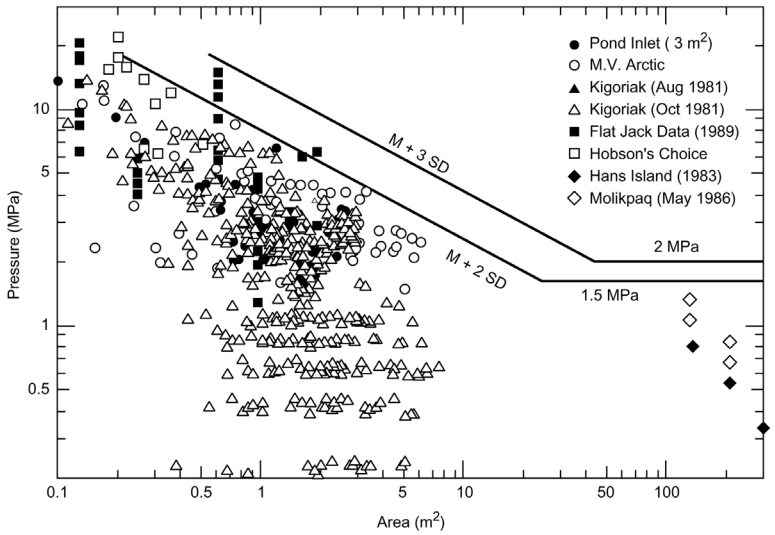

Figure 6-5. plots of effective pressures measured during small- and medium-scale tests, ship ramming, and large-scale field monitoring of ice forces versus nominal contact area. (1 MPa × 145 = 1 psi.)

(4) *Empirical Approach.* Figure 6-5 shows plots of effective pressures measured during small- and medium-scale tests, ship ramming, and large-scale field monitoring of ice forces versus nominal contact area (Masterson and Frederking 1993). Others have also compiled the so-called pressure-area plots(Iyer 1988, Metge et al. 1988, Sanderson 1988). In plotting these data, no regard is given to the speed of indentation into the ice. There is a large scatter in the data on effective pressures for contact areas less than 5 m^2, and this can be attributed to variations in indentation speed. The results of small-scale tests show that there is a decrease in effective pressure with increasing indentation speed, even when the contact area is kept constant (Sodhi 1991, 2001). Lack of scatter in the data for effective pressure for areas greater than 100 meters^2 (1076 feet^2) can be attributed to brittle crushing having been active at high indentation speeds and the creep buckling of floating ice sheet against wide structures preventing the development of high indentation pressure at low ice speeds (Blanchet 1998). The effective pressure, measured during crushing of first-year ice against the 100-meter-wide (328-foot-wide) Molikpaq structure at ice speeds greater than 100 mm s^{-1} (0.328 ft s^{-1}), was in the range of 1 to 2.5 MPa (145 to 363 psi) (Wright et al. 1986, Wright and Timco 1994). Effective pressure in the range of 1–3 MPa (145 to 435 psi) have also been measured on indentors during small-scale tests in the same velocity range (Sodhi 1992, 2001). These two observations indicate that, when continuous brittle crushing

is active, the effective pressure is independent of the nominal contact area. Because high contact pressure can act over a small area resulting from ductile deformation of ice, the trend in the upper bound of effective pressure versus contact area (Figure 6-5) shows a decrease in effective pressure with increasing contact area. Though this trend is known as a scale effect in the literature, the real reason for the decrease in effective pressure with increasing contact area is the possibility of high pressure developing over a small area because of ductile deformation and crushing of the ice in the brittle mode over a large contact area or high aspect ratio (D/h).

(*a*) Two lines in Figure 6-5, labeled as M+2SD and M+3SD, signify trend lines of mean (M) plus two and three standard deviations (SD) of the data, respectively. These are given by:

$$\text{M+2SD: } p(\text{MPa}) = 8.1\,A^{-0.5} \text{ for } 0.1\ \text{m}^2 < A < 29\ \text{m}^2, \text{ and } p = 1.5 \text{ MPa for } A > 29\ \text{m}^2, \quad (6\text{-}12)$$
$$(\text{M+2SD: } p(\text{psi}) = 1175\,A^{-0.5} \text{ for } 1\ \text{ft}^2 < A < 312\ \text{ft}^2, \text{ and } p = 217.5 \text{ psi for } A > 312\ \text{ft}^2)$$

$$\text{M+3SD: } p(\text{MPa}) = 13\,A^{-0.5} \text{ for } 0.1\ \text{m}^2 < A < 42\ \text{m}^2, \text{ and } p = 2 \text{ MPa for } A > 42\ \text{m}^2. \quad (6\text{-}13)$$
$$(\text{M+3SD: } p(\text{psi}) = 1885\,A^{-0.5} \text{ for } 1\ \text{ft}^2 < A < 452\ \text{ft}^2, \text{ and } p = 290 \text{ psi for } A > 452\ \text{ft}^2)$$

(*b*) Both of these equations have been recommended in API (1995). The recommended pressures in the Canadian codes for offshore structures (CSA 1992) are similar. A designer needs to choose the design pressure either higher or lower than the values obtained from Equations 6-12 or 6-13, depending on location of the structure. For example, the Molikpaq structure and its structural components have been designed using pressures given by Equation 6-12 with no visible local damage to the structure, whereas the ice pressure measured on subarctic regions such as Cook Inlet have been less than the pressures given by Equation 6-12.

c. Bending Failure.

(1) *Sloping Structure.* When a floating ice sheet moves against an upward or downward sloping structure, the sheet is pushed either up or down, and breaks by bending into blocks. As the ice sheet continues to be pushed up or down, the broken slabs are further broken into slabs that are typically 4 to 8 times the ice thickness. The force on the structure is limited by the amount required to fail the ice sheet in bending and to overcome the weight and frictional forces of the broken ice blocks. If the structure is narrow, the broken pieces of ice may be able to go around the structure. For wide structures, the broken pieces of ice either ride up to clear over the top of the structure or forms an ice rubble mound. Procedures to estimate ice forces on sloping and conical structures are given in textbooks (Ashton 1986, Cammaert and Muggerdige 1988, Sanderson 1988).

(*a*) API (1995) gives equations for determining the ice forces on a sloping structure, where the broken ice pieces are assumed to ride up the sloping surface and fall off into the water on the other side. Figure 6-6 shows forces during an interaction of a floating ice sheet of thickness h being pushed against a wide sloping surface at an angle α with the horizontal. If the ice blocks are lifted up a height z along the sloping surface, the weight of the broken ice sheet on the sloping surface has a magnitude per unit width of $W=\rho_i g h z/\sin\alpha$, where $\rho_i g$ is the specific weight of ice, and h is the ice thickness. The normal force per unit width on the surface is $N=W\cos\alpha$, and the tangential force along the surface is μN, where μ is the coefficient of friction between the

surface and the ice. As shown in Figure 6-6, the force T acting between the broken ice on the sloping surface and the top of the floating ice sheet has a magnitude per unit width of $T=W(\sin\alpha + \mu\cos\alpha)$.

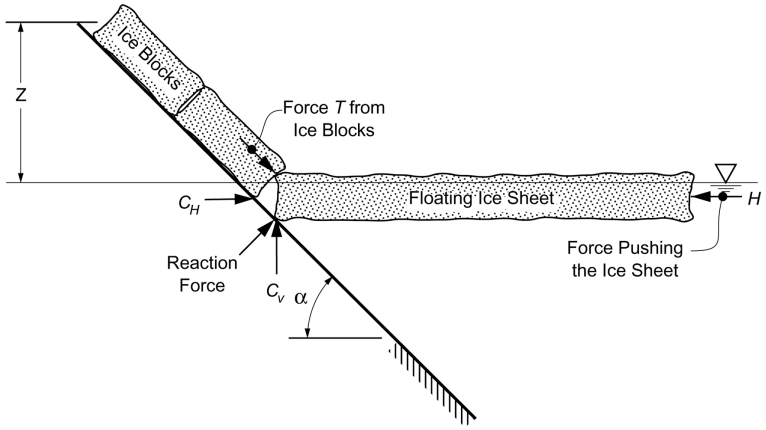

Figure 6-6. forces during an interaction of a floating ice sheet of thickness *h* being pushed against a wide sloping surface at an angle α with the horizontal.

(*b*) The reaction force (Figure 6-6) acting on the contact between the sloping structure and the advancing ice sheet has components C_H and C_V in the horizontal and vertical directions, respectively. The total horizontal force per unit width is given by $C_H + T\cos\alpha$. As the structure pushes the advancing ice sheet up, the vertical force acting at the end of the ice sheet has a magnitude per unit width equal to $C_V - T\sin\alpha$.

(*c*) Under the assumption that there is no moment acting on the floating ice sheet, the vertical force component C_V per unit width required to break the floating ice sheet and push it up is given by:

$$C_V = \frac{\sigma h^2 + 6\ell e^{-\frac{\pi}{4}} T\sin\alpha + Th\cos\alpha}{6\ell e^{-\frac{\pi}{4}} - h\tan(\alpha + \arctan\mu)}, \qquad (6\text{-}14)$$

where

σ = flexural strength of ice sheet
h = ice thickness
α = angle between the sloping surface and the horizontal
ℓ = $[Eh^3/\{12(1-\nu^2)\rho_w g\}]^{1/4}$ (the characteristic length of floating ice sheet)
E = effective elastic modulus of ice
ν = Poisson's ratio of ice
$\rho_w g$ = specific weight of ice.

For typical bending rates, the effective elastic modulus of freshwater ice is in the range of 1–3 GPa (1.45×10^5 to 4.35×10^5 psi), and Poisson's ratio is about 1/3. The range of the coefficient of friction between ice and a structure is between 0.1 for freshly coated surfaces and 0.5 for

rusty, rough surfaces. There are, at present, no guidelines available for the coefficient of friction on rough surfaces or on riprap protected surfaces.

(*d*) The horizontal force C_H per unit width from the structure on the ice sheet is

$$C_H = C_V \tan(\alpha + \arctan \mu) \tag{6-15}$$

The total force H per unit width generated during the interaction to break the ice sheet at a distance away from the contact zone and to push the broken ice block along the sloping surface is given by:

$$H = C_H + T\cos\alpha.$$

Besides other parameters, the total horizontal force on a sloping structure of width D is composed of an icebreaking force proportional to $\sigma h^2 D/\ell$ and an ice ride up force proportional to $\rho_i g h z D$. For narrow structures, the ice breaking component is greater than ice ride up component, whereas the opposite is true for wide structures. Using the above two-dimensional formulation to estimate ice force on a sloping structure gives an order of magnitude of forces, which can be compared to estimates of ice force from other failure modes.

(*e*) The above formulation does not take into account non-simultaneous and incomplete contact between the edge of an ice sheet and a wide structure, as is observed in small-scale tests (Izumiyama et al. 1992, Kovacs and Sodhi 1988). If broken ice pieces accumulate above and below the water surface near the ice–structure contact, the estimate of ice forces should take into account the effect of forces acting on the top and bottom surfaces of the advancing ice sheet (Määttänen and Hoikannen 1990, Croasdale and Cammaert 1993).

(2) *Conical Structure.* There are several methodologies to estimate the ice forces on a conical structure: the elasticity method (e.g., Nevel 1992), the plasticity method (e.g., Ralston 1977, 1980; Izumiyama et al. 1992; Lau 2001), and the results of model tests. Some of these methodologies are briefly presented in API (1995). Several reviews of the literature on the ice forces on conical structures have been presented (Croasdale 1980, Wessels and Kato 1988), and theoretical and experimental results have also been compared (Chao 1992, Wang et al. 1993). Equation 6-15 has also been used to estimate the ice forces on a conical structure by the assuming the width of the conical structure to be $\pi(R+x)$, R being the waterline radius of the conical structure, and $x = \sqrt{2}(\pi/4)\ell$, where ℓ is the characteristic length of floating ice sheets (Croasdale 1980).

(3) *Indentation at High Speeds*. The interaction of a slowing moving ice sheet with a narrow sloping structure usually results in bending failure, resulting in large ice blocks in comparison to their ice thickness. However, when the speed of the moving ice sheet is large, the failure mode changes to shearing or crushing, resulting in small broken ice pieces. Both modes of ice failure against sloping structures have been observed in the field (Neill 1976, Lipsett and Gerard 1980) as well as during small-scale tests in the laboratory (Haynes et al. 1983, Sodhi 1987). This observation implies that ice may fail in crushing, instead of the expected bending, while moving towards a sloping structure at high speeds.

c. Buckling Failure. The ice force on a vertical structure may be limited by the buckling of a floating ice sheet. It depends on the properties of the ice sheet, the width of structure, and the boundary conditions at the ice–structure interface. The boundary conditions along the ice–structure contact line may be defined as rigid, if the ice sheet is frozen to the structure, preventing vertical displacement and rotation. They may be defined as hinged if the ice sheet is allowed to rotate, but is prevented from vertical displacement. And they may be described as free if the ice sheet can displace vertically without encountering any resistance and rotate freely. Discussions of the elastic buckling of beams and plates are given in textbooks and review papers (Hetenyi 1946, Michel 1978, Sodhi and Nevel 1980, Ashton 1986, Cammaert and Muggeridge 1988)

(1) *Elastic Buckling.* For a beam of floating ice sheet, the elastic buckling force (Hetenyi 1946) is given by

$$F_b = \alpha \rho_w g B L_b^2 \tag{6-16}$$

where

α = factor that depends on the ratio of beam length to the characteristic length and the boundary conditions at the ends of the beam.
$\rho_w g$ = specific weight of water,
B = beam width,
L_b = characteristic length of the floating ice beam and is equal to $[Eh^3/(12\rho_w g)]^{1/4}$
h = ice thickness
E = modulus of elasticity of ice.

For beam lengths much longer than the characteristic length of a floating ice beam, the factor α is either equal to 1 if one or both ends of the beam are free, or equal to 2 if one or both ends of the beam are either rigid or hinged (Sodhi and Nevel 1980).

(*a*) The elastic buckling forces of wedge-shaped, semi-infinite ice sheets is given by

$$F_p = [C+D/(R/L)]\rho_w g B L^2 \tag{6-17}$$

where

C and D = coefficients given in Table 6-1 for three boundary conditions and five wedge angles in the range of 2 to 180°
R = radius of the structure at the contact line
$\rho_w g$ = specific weight of water
B = structure width
L = characteristic length of the floating ice sheet and is equal to $[Eh^3/\{12(1-\nu^2)\rho_w g\}]^{1/4}$,
h = ice thickness
E = modulus of elasticity of ice.

A recommended value of the characteristic length of freshwater ice $L = 16h^{3/4}$, and that of sea ice $L = 13h^{3/4}$, where L and h are in meters (Gold 1971).

Table 6-1
Coefficients for the estimation of buckling force

	Boundary conditions at the ice–structure contact line					
	Free		Hinged		Rigid	
Angle	C	D	C	D	C	D
2°	0.96	0.80	2.11	2.76	2.57	4.47
30°	1.00	0.82	2.20	3.11	2.55	4.70
90°	0.95	1.01	2.04	3.78	2.35	5.34
150°	0.84	1.36	1.81	4.30	2.08	5.83
180°	0.81	1.66	0.75	4.67	2.04	6.05

(*b*) Experimental studies on the buckling of floating ice sheet indicate that the non-dimensional buckling forces fall between those for free and hinged boundary conditions at the contact line (Sodhi et al. 1983). For tests in which the boundary condition was simulated as hinged, the experimental and theoretical results are close to each other (Sodhi and Adley 1984).

(2) *Creep Buckling.* For creep buckling, a floating ice sheet is considered to become unstable when the vertical deflections of the ice sheet suddenly increase after a long period of slow in-plane deformation. In a series of finite element analyses of an ice sheet being pushed slowly against a 152-meter-diameter (500-foot-diameter)structure, the results show that the ice sheet deforms slowly in the vertical direction until a critical time when large deformations suddenly occur in the vicinity of the structure (Luk 1990). The critical time t_{cr} at which large deformations take place can be estimated as

$$t_{cr} = 0.36\, D/v, \tag{6-18}$$

where D is the width of the structure, and v is the ice velocity. For an elastic modulus of 4.83 GPa (7.0×10^5 psi), a Poisson's ratio of 0.3, and a creep exponent of 3, the results of finite element analysis show that the following relationship between the effective pressure p and the critical time t_{cr} is

$$(p/\text{MPa}) = (7.07\ \text{days}/t_{cr})^{0.336}. \tag{6-19}$$

d. Floe Splitting. When a floating ice floe impacts and crushes against a structure, the floe may split up after some amount of crushing. The ice–structure interaction results in deceleration of the ice floe, which creates a distributed inertia body force per unit volume over the entire floe. Depending on the geometry of the structure, the ice crushing in the contact zone produces a longitudinal force as well as a pair of self-equilibrating transverse forces, which are a fraction β of

the longitudinal force. Under the assumption that the linear elastic fracture mechanics is applicable, the critical force F_{sp} to split a square floe of length λ and of thickness h is given by

$$F_{sp} = 3.3\ h\ K_{1c}\ \lambda^{1/2}, \tag{6-20}$$

where K_{1c} is the fracture toughness of ice (Bhat 1988). Similar ice splitting forces can also be estimated for different floe width-to-length ratios and different values of β (Dempsey et al. 1993). The fracture toughness of freshwater and saline ice through small-scale and large-scale measurements is in the range of 50 to 250 kPa $m^{1/2}$ (0.007 to 0.036 ksi $in^{0.5}$) (Dempsey et al. 1999a,b). Small-scale tests were conducted with freshwater ice floes of different thicknesses and widths, and those experimental results were found to be close to the theoretical forces obtained from finite element analysis using linear elastic fracture mechanics (Sodhi and Chin 1995).

e. Structures Going Through Broken Ice Cover. When a structure goes through a broken up ice cover having a depth t_k and a height t_s from the water surface, the force F per unit width (Mellor 1980) is given by

$$F = \frac{1}{2}\frac{1+\sin\phi}{1-\sin\phi}(1-n)\left[\rho_i g t_s^2 + (\rho_w - \rho_i) g t_k^2\right] + 2c\sqrt{\frac{1+\sin\phi}{1-\sin\phi}}(t_s + t_k), \tag{6-21}$$

where

ϕ = angle of internal friction
c = cohesive strength of rubble ice
n = porosity of rubble ice
$\rho_i g$ = specific weight of ice
$\rho_w g$ = specific weight of water.

6-5. Forces Limited by the Momentum of an Ice Feature

a. When an isolated ice feature impacts a structure, it may come to rest, deflect, or rebound from the structure. The interaction forces during an impact may be computed from the equations of momentum and energy of the two colliding bodies (Goldsmith 1960). Because the rate of indentation during an ice impact is usually high, brittle crushing of ice is expected to take place in the contact area, which depends on the local geometry of the ice feature and the structure.

b. For a head-on collision in which a moving ice feature comes to a stop against a structure, the initial kinetic energy is dissipated to crush a certain volume V of ice at an effective pressure of p_e to give

$$Mv^2/2 = p_e V, \tag{6-22}$$

where M is the mass of the ice feature including the added mass of water, and v is its velocity. The depth d and the area A of ice crushing can be calculated from the estimated volume V of the crushed ice and the local geometry of the ice feature and the structure. The interaction force can now be estimated as $F = p_e A$.

c. An eccentric impact (Figure 6-7) will rotate the ice floe, and the ice feature will retain a portion of the initial kinetic energy after the impact. By equating the initial kinetic energy to the sum of remaining kinetic energy and dissipation of energy during ice crushing, the following relationship can be shown under the assumption of brittle crushing (Nevel 1986):

$$\frac{Mv^2}{2} = \frac{Mv^2}{2}\left[\frac{(Y/R)^2}{1+(R_g/R)}\right] + (1+\mu\tan\beta)\,p_e V \tag{6-23}$$

where

M = mass of ice feature, including the added mass of water
v = ice feature velocity
Y = eccentricity of the center of gravity from the point of impact
R = distance of the center of gravity from the point of impact
R_g = radius of gyration of the ice feature about the vertical axis through its center of gravity
μ = ratio of tangential force to normal force in the contact area
β = angle of local contact geometry ($\beta = 0$ for head-on impact
p_e = effective pressure to crush ice
V = volume of ice crushed.

For a particular impact situation, the volume of ice crushed during an impact is estimated, and then the depth d and the area A of ice crushed are estimated from the local contact geometry. Lastly, the interaction force is estimated as $F = p_e A$.

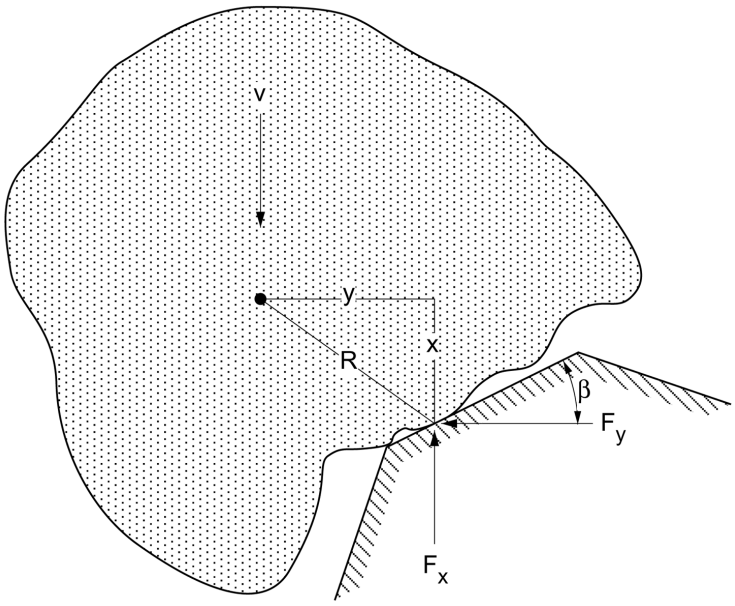

Figure 6-7. An eccentric impact that will rotate the ice floe, allowing the ice feature to retain a portion of the initial kinetic energy after the impact.

6-6. Canadian and American Codes

a. To estimate dynamic ice force F on bridge piers resulting from moving ice, CSA (2000) and AASHTO (1994) codes specify the following:

F = lesser of the F_c or F_b for $D/h<6$

and

$F = F_c$ for $D/h>6$

where

F_c = $C_a pDh$ (horizontal force in when ice floes fail by crushing over full width of the pier)
F_b = $C_n ph^2$ (horizontal force in when ice floes fail in bending against a sloping pier)
D = the pier width
h = the ice thickness
C_a = $(5h/D+1)^{0.5}$ (to account for the aspect ratio effect found in small-scale identation tests)
C_n = $0.5 \tan(\alpha+15°)$
α = slope of the pier from the downstream horizontal (<75°)
p = effective ice crushing pressure for which following values have been recommended.

0.7 MPa (101.5 psi)	Ice breaks up at melting temperature and is somewhat disintegrated.
1.1 MPa (159.5 psi)	Ice breaks up or moves at melting temperature, but the ice moves in large floes and is internally sound.
1.5 MPa (217.5 psi)	Ice breaks up or moves at temperatures considerably below its melting point. Even higher pressures are recommended for ice temperatures 2 or 3°C (35.6 or 37.4ºF) below melting temperatures.

b. Further, these codes recommend reducing the dynamic ice force F by 50% of the values derived above for piers in small streams where it is unlikely to encounter large-size floes.

c. For oblique impacts, readers should see the CSA (2000) and AASHTO (1994) codes.

d. It should be mentioned here that the above-recommended values of effective crushing pressure have been obtained from measurements of ice forces on two bridge piers in Alberta, Canada (Lipsett and Gerard 1980). These recommended values for effective pressure for wide structures are the same as those given by Equation 6-12. For narrow structures, the factor C_a accounting for the aspect ratio effect raises the effective pressure to higher values, similar to given by Equation 6-12 for nominal contact area less than 29 meters^2 (312 feet^2).

6-7. Vertical Ice Forces

a. Marine structures that become frozen into an ice sheet are subjected to vertical ice forces as the ice sheet responds to changes in water level. Typically, the uplifting load resulting from changes in water level governs the design of light-duty, pile-founded docks common in marinas. Thus, reducing the vertical ice loads by active (bubblers or water jet) or passive (pile jacket or low-adhesive coatings) means will directly lead to lower costs for such structures. Theoretical estimates of vertical ice loads in the literature (e.g., Ashton 1986) depend on the assumed mode of ice failure, which is often difficult to ascertain for a particular situation. For instance, Muschell and Lawrence (1980) conducted pull-out tests after freezing a conventional capped pipe pile (filled with air) and another similar pile filled with vermiculite insulation, and found a 30% reduction in vertical ice force. In a conventional capped pipe pile, a thermal convection cell develops, resulting in freezing of thicker ice adjacent to the pile. The insulation-filled pipe interrupted this heat transfer, reducing the localized ice thickening and thus yielding a 30% reduction in pull-out force. An epoxy coating was applied to both air-filled and vermiculite-filled piles, which resulted in a net load reduction of 35 and 70%, respectively. Frederking and Karri (1983) used polyethylene and PVC piles with an average reduction in failure stress of 70% compared with similar size wooden piles used in a previous study (Frederking 1979). It was observed that the failure occurred at the ice/ice interface in the case of conventional piles, whereas the relative movement in the case of epoxy coated or plastic piles was at the pile/ice interface.

b. While reviewing the results of pull out tests in the literature, Zabilansky (1998) noted that the researchers used the following three test techniques to conduct a test.

(1) *Socket.* A hole was drilled through part of an ice sheet, a pile was placed in the counter-bored hole, and the void between the ice and the pile was filled with water. This test technique measured the anchoring capacity of the pile, which is not representative of the marina application.

(2) *Confined.* Most of these tests were conducted using a testing machine to extract a pile out a block of ice. Muschell and Lawrence (1980) conducted a series of tests on a lake. They froze a pile into an ice sheet by placing it in a hole cut in the ice sheet and allowing the annulus water between the pile and the ice sheet to freeze. The test was conducted about a week later by jacking the pile out while reacting the parent ice sheet. In these tests, the reaction ring or plate was slightly larger than the pile, resulting in shear failure of ice adjacent to the pile.

(3) *Unconfined.* A pile was either placed into a tank of water during freezing of an ice sheet or frozen into an ice sheet on a lake. The tests were conducted by pulling out the pile while reacting against either the edge of a tank or a support frame placed on top of the ice sheet. This mode of loading subjected the ice sheet to both bending and shear stresses, and was more representative of the observed failure mode in the field.

c. Zabilansky (1998) compiled the data from the pull-out tests with wooden piles conducted at CRREL (Zabilansky 1986) and unconfined tests reported in the literature. He plotted the shear

stress (force/circumferential contact area) with respected to the ratio of pile diameter to ice thickness, as shown in Figure 6-8. A line of best fit through the data is given by:

$$\sigma = 300/(d/h)^{0.} \tag{6-24}$$

The equation for the pull out force is given as:

$$P = \sigma\pi dh = 300\pi h^{1.6} d^{0.4} \tag{6-25}$$

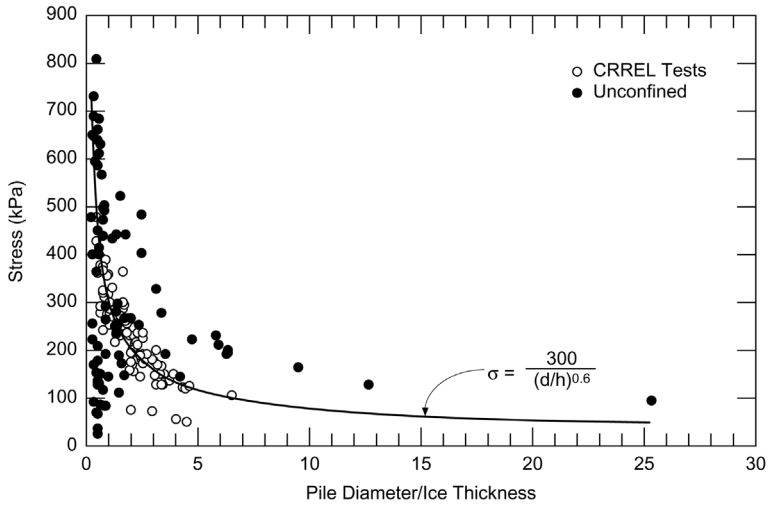

Figure 6-8. Failure shear stress vs. ratio of pile diameter to ice thickness. (1 kPa × 0.145 = 1 psi.)

6-8. Summary

This Chapter estimates ice forces on the basis of ice mechanics for its failure in various modes, as well as on empirical values of effective pressure measured on full-scale structures. For ice crushing, which induces the highest effective pressure on a structure, the effective pressure depends on the indentation speed and the aspect ratio (D/h). Most of the codes take these factors into account for estimating ice forces on structures. When an ice sheet fails in modes other than crushing, the effective pressure is generally less.

6-9. References

Croasdale (1980)
Croasdale, K.R. (1980) Ice forces on fixed, rigid structures. In *IAHR Working Group on Ice Forces on Structures* (Ed. T. Carstens), U.S. Army Cold Regions Research and Engineering Laboratory, Special Report 80-26, pp. 34–106.

Drouin and Michel (1974)
Drouin, M., and B. Michel (1974) Pressures of Thermal Origin Exerted by Ice Sheets upon Hydraulic Structures, Draft Translation 427, U.S. Army Cold Regions Research and Engineering Laboratory, Hanover, NH.

Ettema and Urroz-Aguirre (1991)
Ettema, R., and G.E. Urroz-Aguirre (1991) Friction and cohesion in ice rubble reviewed, *Proceedings of the 6th Internation Specialty Conference on Cold Regions Engineering, U.S. Army Cold Regions Research and Engineering Laboratory, Hanover, NH*, pp. 316–325.

Haynes et al. (1983)
Haynes, F. D., D. S. Sodhi, K. Kato, and H. Hirayama (1983) Ice forces on model bridge piers. CRREL Report 83-19, U.S. Army Cold Regions Research and Engineering Laboratory, Hanover, N.H.

Kjeldgaard and Carstens (1980)
Kjeldgaard, J.H., and T. Carstens (1980) Thermal Ice Forces, in Special Report 80-26, U.S. Army Cold Regions Research and Engineering Laboratory, Hanover, NH, pp 1–33.

Korzhavin (1962)
Korzhavin, K.M. (1962) Action of Ice on Engineering Structures, Translation 260, U.S. Army Cold Regions Research and Engineering Laboratory, Hanover, NH.

Kovacs and Sodhi (1988)
Kovacs, A., and D.S. Sodhi (1988) Onshore ice pile-up and ride-up: Observations and theoretical assessment, *Arctic Coastal Processes and Slope Protection Design*, ASCE Technical Council on Cold Regions Engineering Monograph (A.T. Chen and C.B. Leidersdorf, Ed), pp. 108–142.

Michel (1970)
Michel, B. (1970) Ice Pressures on Engineering Structures. Monograph III-B1b, U.S. Army Cold Regions Research and Engineering Laboratory, Hanover, NH.

Sodhi and Nevel (1980)
Sodhi, D.S. and Nevel, D.S. (1980) A review of buckling analyses of ice sheets, *IAHR Working Group on Ice Forces on Structures* (Ed. T. Carstens), Special Report 80-26, U.S. Army Cold Regions Research and Engineering Laboratory, Hanover, NH, pp. 131–146.

AASHTO (1994)
American Association of State Highway and Transportation Officials (1994) AASHTO LFRD Bridge Design Specifications, 444 North Capitol Street, N.W., Suite 249, Washington, D. C. 20001.

API (1995)
American Petroleum Institute (1995) Recommended Practice for Planning, Designing, and Constructing Structures and Pipelines for Arctic Conditions, 2nd Edition, API Publications, 1220 L Street N.W., Washington, DC 20005.

Ashton (1986)
Ashton, G.D. (Editor) (1986) *Lake and River Ice Engineering*, Water Resources Publications, Littleton, Colorado.

Banke and Smith (1973)
Banke, E.G. and S.D. Smith (1973) Wind stress on Arctic sea ice, *Journal of Geophysical Research*, **78**(35): 7871–7882.

Belkov (1973)
Belkov, G. (1973) Instructions for Determining Ice Loads on River Structures (SN 76-66), National Research Council of Canada, Technical Translation 1663.

Bhat (1988)
Bhat, S.U. (1988) Analysis of splitting of ice floes during summer impacts, *Cold Regions Science and Technology*, **5**(1): 53–63.

Blanchet (1998)
Blanchet, D. (1998) Ice loads from first-year ice ridges and rubble fields, *Canadian Journal of Civil Engineering*, **25**: 206–219.

Cammaert and Muggeridge (1988)
Cammaert, A.B. and D.B. Muggeridge (1988) *Ice Interaction with Offshore Structures*, Van Nostrand Reinhold, New York.

Carter et al. (1998)
Carter, D., D.S. Sodhi, E. Stander, O. Caron, and T. Quach (1998) Ice thrust in reservoir, *Journal of Cold Regions Engineering*, **12**(4): 169–183.

Chao (1992)
Chao, J.C. (1992) Comparison of sheet ice load prediction methods and experimental data for conical structures, *OMAE-92*, Vol. IV, pp. 183–193.

Cole (1995a)
Cole, D.M. (1995a) Cyclic loading of saline ice. *Philosophical Magazine A*, **72**(1): 209–229.

Cole (1995b)
Cole, D.M. (1995b) Model for the anelastic straining of saline ice subjected to cyclic loading. *Philosophical Magazine A*, **72**(1): 231–248.

Comfort and Abdelnour (1994)
Comfort, G., and R. Abdelnour (1994) Field measurements of ice loads: Thermal loads on hydroelectric structures. Proceedings, 1994 Canadian Dam Safety Association, Winnipeg, Manitoba, Canada, pp 35–51.

Comfort and Armstrong (2001)
Comfort, G., and T. Armstrong (2001) Static ice loads on dams: Project update, Canadian Dam Association Bulletin.

Comfort et al. (2000a)
Comfort, G., Y. Gong, and S. Singh (2000a) Predicting static ice loads on dams, *Proceedings, 15th International Symposium on Ice, Gdansk, Poland*, Volume 1, pp. 135–144.

Comfort et al. (2000b)
Comfort, G., Y. Gong, and S. Singh (2000b) The factors controlling static ice loads on dams, *Proceedings, 15th International Symposium on Ice, Gdansk, Poland*, Volume 1, pp. 189–197.

Cornett and Timco (1996)
Cornett, A.M. and G.W. Timco (1996) Mechanical properties of dry saline ice rubble, *Proceedings of the 6th ISOPE Conference, Los Angeles, Cal., USA*, Vol. II, pp 297–303.

Cox and Weeks (1983)
Cox, G.F.N., and W.F. Weeks (1983) Equations for determining the gas and brine volumes in sea-ice samples, *Journal of Glaciology*, **29**(102): 306–316.

Croasdale and Cammaert (1993)
Croasdale, K.R. and A.B. Cammaert (1993) An improved method for the calculation of ice loads on sloping structures in first-year ice, *Presented at the 1st International Conference on Development of the Russian Arctic, St. Petersburg, Russia, November, 1993*.

Croasdale et al (1977)
Croasdale, K.R., N.R. Morgenstern, and J.B. Nuttall (1977) Indentation tests to investigate ice pressures on vertical piers, *Journal of Glaciology*, **81**:301–312.

CSA (1988)
Canadian Standards Association (1988) Design of Highway Bridges, A National Standard of Canada, CAN/CSA-S6-88, Rexdale, Ontario, Canada.

CSA (2000)
Canadian Standards Association (2000) Design of Highway Bridges, A National Standard of Canada, CAN/CSA-S6-88, Rexdale, Ontario, Canada.

CSA (1992)
Canadian Standards Association (1992) General Requirements, Design Criteria, the Environment and Loads, Codes for the Design, Construction and Installation of Fixed Offshore Structures, CSA-S471, Rexdale, Ontario, Canada.

Dempsey et al. (1993)
Dempsey, J.P., S.J. DeFranco, D. Blanchet, and A. Prodanovic (1993) Splitting of ice floes, *Proceedings, 12th International Conference on Port and Ocean Engineering Under Arctic Conditions, Hamburg, Germany*, vol. I, p. 17–22.

Dempsey et al. (1999a)
Dempsey, J. P., S. J. Defranco, R. M. Adamson, and S. V. Mulmule (1999a) Scale effects on the in-situ tensile strength and fracture of ice. Part I: Large grained freshwater ice at Spray Lakes Reservoir, Alberta, *International Journal of Fracture Mechanics*, **95**: 325–345.

Dempsey et al. (1999b)
Dempsey, J. P., R. M. Adamson, and S. V. Mulmule (1999b) Scale effects on the in-situ tensile strength and fracture of ice. Part II: First-year sea ice at Resolute, N.W.T., *International Journal of Fracture Mechanics*, **95**: 347–366.

Fransson (1988)
Fransson, L., (1988) Thermal Ice Pressure on Structures in Ice Covers, Ph.D. Thesis, Lulea University of Technology, Sweden.

Frankenstein and Garner (1967)
Frankenstein, G. and R. Garner (1967) Equations for determining the brine volume of sea ice from –0.5° to –22.9°C, *Journal of Glaciology*, **6**(48): 943–944.

Frederking (1979)
Laboratory tests on down-drag loads developed by floating ice covers on vertical piles, *POAC'79, Port and Ocean Engineering under Arctic Conditions, Norwegian, Institute of Technology*.

Frederking and Karri (1983)
Frederking, R.F., and J. Karri (1983) Effects of pile material and loading state on adhesive strength of piles in ice, *Canadian Geotechnical Journal*, **20**: 673–680.

Frederking et al. (1990)
Frederking, R., I.J. Jordaan, and J.S. McCallum (1990) Field tests of ice indentation of medium scale Hobson's Choice Ice Island, 1989, *Proceedings, 10th IAHR Symposium on Ice, Espoo, Finland*, vol. 2, pp. 931–944.

Gagnon (1998)
Gagnon, R.E. (1998) Analysis of visual data from medium scale indentation experiments at Hobson's Choice Ice Island, *Cold Regions Science and Technology*, **28**: 45–58.

Gold (1971)
Gold, L. W. (1971) Use of ice covers for transportation, *Canadian Geotechnical Journal*, **8**: 170–181.

Goldsmith (1960)
Goldsmith, W. (1960) *Impact: the Theory and Physical Behaviour of Colliding Solids*, Edward Arnold (Publishers), London.

Hetenyi (1946)
Hetenyi, M. (1946) *Beams on Elastic Foundation*, The University of Michigan Press, Ann Arbor, Michigan.

Izumiyama et al (1992)
Izumiyama, K., H. Kitagawa, K. Koyama, and S. Uto (1992) A numerical simulation of ice-cone interaction, *IAHR-92*, Vol, 1, pp. 188–199.

Iyer (1988)
Iyer, S. H. (1988) A state-of-the-art review of local ice loads for the design of offshore structures, *Proceedings, 9th International Symposium on Ice, Sapporo, Japan*, Vol. 2, pp. 509–566.

Jefferies and Wright (1988)
Jefferies, M.G., and W.H. Wright (1988) Dynamic response of "Molikpaq" to ice–structure interaction. In *Proceedings, 7th International Conference on Offshore Mechanics and Arctic Engineering (OMAE), Houston, Texas,* Vol. IV, p. 201–220.

Joensuu and Riska (1989)
Joensuu, A., and K. Riska (1989) Contact between ice and structure (in Finnish), Laboratory of Naval Architecture and Marine Engineering, Helsinki University of Technology, Espoo, Finland, Report M-88.

Kry (1978)
Kry, P.R. (1978) A statistical prediction of effective ice crushing stress on wide structure. In *Proceedings, 4th IAHR Symposium on Ice Problems, Lulea, Sweden*, p. 33–47.

Lau (2001)
Lau, M. (2001) A three dimensional discrete element simulation of ice sheet impacting a 60° conical structure. In *Proceedings, 16th International Conference on Port and Ocean Engineering Under Arctic Conditions, Ottawa, Canada*, Vol. I, p. 431–440.

Lipsett and Gerard (1980)
Lipsett, A.W., and R. Gerard (1980) Filed measurements of ice forces on bridge piers, 1973–79, Alberta Research Council, Edmonton, Alberta, Canada, Report No. SWE 80–3.

Løset and Sayed (1993)
Løset, S. and M. Sayed (1993) Proportional strain tests of freshwater ice rubble, *Journal of Cold Regions Engineering*, **7**(2): 44–61.

Luk (1990)
Luk, C. H. (1990) Creep buckling analysis of floating ice sheets moving against a vertical cylindrical structure, *Proceedings 9th Offshore Mechanics and Arctic Engineering, Houston, Texas*, Vol. 4, pp. 103–110.

Määttänen and Hoikkanen (1990)
Määttänen, M., and J. Hoikkanen (1990) The effect of ice pile-up on the ice force of a conical structure, *IAHR-90*, Vol. 2, pp. 1010–1021.

Masterson and Frederking (1993)
Masterson, D.M., and R.M.W. Frederking (1993) Local contact pressures in ship/ice and structure/ice interaction, *Cold Regions Science and Technology*, **3**(4): 305–321.

Masterson et al. (1999)
Masterson, D.M., P.A. Spencer, D.E. Nevel, and R.P. Nordgren (1999) Velocity effects from multi-year ice tests, *Proceeding, 18th International Offshore Mechanics and Arctic Engineering Conference, St. John's, Newfoundland, Canada*, OMAE99/P&A1127.

Mellor (1980)
Mellor, M. (1980) Ship resistance in thick brash ice, *Cold Regions Science and Technology*, **3**(4): 305–321.

Metge (1976)
Metge, M. (1976) Thermal cracks in lake ice. Ph. D. thesis, Queen's University, Kingston, Ontario, Canada.

Metge et al. (1988)
Metge, M., D. Masterson, K.R. Croasdale, N. Allyn, and S. Hotzel (1988) A large scale ice-structure interaction data base, *Proceedings, 9th International Symposium on Ice, Sapporo, Japan*, Vol. 2, pp. 567–584.

Michel (1978)
Michel, B. (1978) *Ice Mechanics*. Laval University Press, Quebec, PQ, Canada.

Michel and Toussaint (1977)
Michel, B., and N. Toussaint (1977) Mechanisms and theory of indentation of ice plates, *Journal of Glaciology*, **19**(81): 285–300.

Montgomery et al. (1984)
Montgomery, C.J., R. Gerard, W.J. Huiskamp, R.W. Kornelson (1984) Application of ice engineering to bridge design standards, *Proceedings, Cold Regions Engineering Specialty Conference, 4–6 April, 1984*, Canadian Society for Civil Engineering, Montreal, Canada, pp. 795–810.

Muschell and Lawrence (1980)
Muschell, J.E., and R.G. Lawrence (1980) Ice uplift on piles: Progress report of water temperature and ice pile adhesion investigations on the Upper Great Lakes, Michigan Sea Grant Program, MICHU-SG-80-506.

Neill (1976)
Neill, C.R. (1976) Dynamic ice forces on piers and piles: An assessment of design guidelines in the light of recent research, *Canadian Journal of Civil Engineering*, **3**(2): 305–341.

Nevel (1986)
Nevel, D.E. (1986) Iceberg impact forces, *Proceedings IAHR Symposium on Ice 1986, Iowa City*, Vol. III, pp. 345–369.

Nevel (1992)
Nevel, D.E. (1992) Ice forces on cones from floes, *IAHR-92*, Vol. 3, pp. 1391–1404.

Ponter et al. (1983)
Ponter, A. R.S., A.C. Palmer, D.J. Goodman, M.F. Ashby, A.G. Evans, and J.W. Hutchinson (1983) The forces exerted by a moving ice sheet on an offshore structure, *Cold Region Science and Technology*, **8**(2):109–118.

Prodanovic (1979)
Prodanovic, A. (1979) Model tests of ice rubble strength, *Proceedings, 5th POAC Conference, Trondheim, Norway*, Vol. 1, pp. 89–105.

Ralston (1977)
Ralston, T.D. (1977) Ice force design considerations for conical offshore structures, *POAC-77*, Vol. II, pp. 741–752.

Ralston (1980)
Ralston, T.D. (1980) Plastic limit analysis of sheet ice on conical structures, *Physics and Mechanics of Ice* (P. Tryde, Ed.), Springer-Verlag, Berlin, pp. 289–300.

Riska (1991)
Riska, K. (1991) Observations of the line-like nature of ship-ice contact, *Proceedings, 11th International Conference on Port and Ocean Engineering Under Arctic Conditions, St. John's, Newfoundland, Canada*, vol. II, p. 785–811.

Rose (1947)
Rose, E. (1947) Thrust exerted by expanding ice sheets, *Transactions of the ASCE*, **112**: 871.

Saeki et al. (1996)
Saeki, H., K.-I. Hirayama, T. Kawasaki, S. Akagawa, K. Kato, K. Kamesaki, K. Saka, and A. Kurokawa (1996) JOIA project of study of ice load, *Proceedings, 13th International Symposium on Ice, Beijing, China*, Vol.1, pp.17–27.

Sanderson (1984)
Sanderson, T. (1984) Thermal ice forces against isolated structures, *Proceedings, IAHR Ice Symposium*, *Hamburg, Germany,* Vol. IV, pp 289–299.

Sanderson (1988)
Sanderson, T.J.O. (1988) *Ice Mechanics: Risks to Offshore Structures*. Graham and Trotman, London.

Sinha et al. (1987)
Sinha, N.K., G.W. Timco, and R. Frederking (1987) Recent advances in ice mechanics in Canada, *Applied Mechanics Review*, **40**(9): 1214–1231.

Sodhi (1987)
Sodhi, D.S. (1987) Dynamic analysis of failure modes of ice sheets encountering sloping structures, *Proceedings, 6th International Offshore Mechanics and Arctic Engineering Conference, Houston, Texas*, Vol. IV, pp. 281–284.

Sodhi (1991)
Sodhi, D.S. (1991) Ice-structure interaction during indentation tests, *Ice-Structure Interaction*: *Proceedings of IUTAM-IAHR Symposium* (S. Jones et al., Ed.). Springer-Verlag, Berlin, pp. 619–640.

Sodhi (1992)
Sodhi, D.S. (1992) Ice-structure interaction with segmented indentors, *Proceedings, 11th IAHR Symposium on Ice 1992, Banff, Alberta, Canada*, vol. 2, pp. 909–929.

Sodhi (1995)
Sodhi, D.S. (1995) An ice-structure interaction model, *Mechanics of Geomaterial Interfaces,* (A. P. S. Selvadurai and M. J. Bolton, Eds.), Elsevier Science B. V., Amsterdam, pp. 57–75.

Sodhi (1998)
Sodhi, D.S. (1998) Nonsimultaneous crushing during edge indentation of freshwater ice sheets, *Cold Regions Science and Technology*, **27**(3): 179–195.

Sodhi (2001)
Sodhi, D.S. (2001) Crushing failure during ice-structure interaction, *Journal of Engineering Fracture Mechanics*.

Sodhi et al. (1983)
Sodhi, D.S., F.D. Haynes, K. Kato, and K. Hirayama (1983) Experimental determination of the buckling loads of floating ice sheets, *Annals of Glaciology*, **4**: 260–265.

Sodhi and Adley (1984)
Sodhi, D.S., and M.D. Adley (1984) Experimental determination of buckling loads of cracked ice sheets, *Proceedings, 3rd Offshore Mechanics and Arctic Engineering, New Orleans, Louisianna*, Vol. 3, pp. 183–186.

Sodhi and Chin (1995)
Sodhi, D.S. and Chin S.N. Chin (1995) Indentation and splitting of freshwater ice floes, *Journal of Offshore Mechanics and Arctic Engineering*, **117**: 63–69.

Sodhi et al. (1998)
Sodhi, D.S., T. Takeuchi, N. Nakazawa, S. Akagawa, and H. Saeki (1998) Medium-scale indentation tests on sea ice at various speeds, *Cold Regions Science and Technology*, **28**: 161–182.

Strilchuk (1977)
Strilchuk, A.R. (1977) Ice pressure measurements, Netserk F-40, 1975–76, Arctic Petroleum Operators Association, APOA Project No. 105-1.

Timco and Frederking (1990)
Timco, G.W., and R.M.W. Frederking (1990) Compressive strength of sea ice sheets, *Cold Regions Science and Technology*, **17**: 227–240.

Timco and O'Brien (1994)
Timco, G.W. and S. O'Brien (1994) Flexural strength equation for sea ice. *Cold Regions Science and Technology,* **22**: 285–298.

Timco et al. (1996)
Timco, G.W., D.A. Watson, G.A. Comfort, and R. Abdelnour (1996) A comparison of methods for predicting thermally-induced ice loads, *Proceedings 13th IAHR Symposium on Ice, Beijing, China*, Vol. 1, pp 241–248.

Wang et al. (1993)
Wang, Z., D.B. Muggeridge, A. Prodonovic, and J.C. Chao (1993) Computation of sheet ice and ridge ice forces on a faceted cone, *POAC-93*, Vol. 2, pp. 627–638.

Weber and Nixon (1992)
Weber, L.J., and W.A. Nixon (1992) Fracture toughness of granular freshwater ice, *Proceedings of the 11th OMAE, Calgary, AL, Canada*, Vol. IV, pp 377–381.

Wessels and Kato (1988)
Wessels, E. and K. Kato (1988) Ice forces on fixed an floating conical structures, *IAHR-88*, Vol. 2, pp. 666–691.

Wright et al. (1986)
Wright, B., G.R. Pikington, K.S. Woolner, and W.H. Wright (1986) Winter ice interactions with an arctic offshore structure, *Proceedings, 8th IAHR Symposium on Ice, Iowa City, Iowa*, vol. II, pp. 49–73.

Wright and Timco (1994)
Wright, B.D., and G.W. Timco (1994) A review of ice forces and failure modes on the Molikpaq, *Proceedings, 12th IAHR Symposium on Ice, Trondheim, Norway,* vol. 2, pp. 816–825.

Xu Bomeng (1981)
Xu Bomeng (1981) Pressure due to expansion of ice sheet in reservoirs, *IAHR Ice Symposium 1981, Quebec City*, pp. 540–550.

Xu Bomeng (1986)
Xu Bomeng (1986) Design value of pressure due to expansion of ice sheet in reservoir, *IAHR Ice Symposium 1986, Iowa City, Iowa*, pp. 231–238.

Zabilansky (1986)
Zabilansky, L.J. (1986) Model study of ice force on a single pier, *IAHR Ice Symposium 1986, Iowa City, Iowa*, Vol. 3, pp 77.

Zabilansky (1998)
Zabilansky, L.J. (1998) Vertical forces and aspect ratio of pile diameter vs. ice thickness, *Proceedings, 14th International IAHR Symposium on Ice, Ice in Surface Waters* (H.T. Shen, Ed), Balkama, Rotterdam, Vol. 2.